miR-132 controls mouse pancreatic beta cell proliferation and survival through the *Pten*/*Akt*/*Foxo3* signaling

Hassan Mziaut[1,2,3], Georg Henniger[4], Katharina Ganss[1,2,3], Sebastian Hempel[4], Steffen Wolk[4], Johanna McChord[4], Kamal Chowdhury[5], Klaus-Peter Knoch[1,2,3], Jürgen Weitz[4], Robert Grützmann[7], Christian Pilarsky[7], Michele Solimena[1,2,3,6]*, Stephan Kersting[7]*

[1] Molecular Diabetology, University Hospital and Faculty of Medicine, TU Dresden, Dresden, Germany

[2] Paul Langerhans Institute Dresden of the Helmholtz Center Munich at the University Hospital and Faculty of Medicine of TU Dresden, Dresden, Germany

[3] German Center for Diabetes Research (DZD e.V.), Neuherberg, Germany

[4] Department of General, Thoracic and Vascular Surgery, Faculty of Medicine, TU Dresden, Dresden, Germany

[5] Max Planck Institute of Biophysical Chemistry, Göttingen, Germany

[6] Max Planck Institute of Molecular Cell Biology and Genetics, Dresden, Germany

[7] Department of Surgery, University of Erlangen, Erlangen, Germany

*Corresponding authors

E-mail: stephan.kersting@uk-erlangen.de; michele.solimena@tu-dresden.de

Tables and Figures: 1/5

Supplemental Tables and Figures: 8/2

Abbreviations

miRNA – microRNA; *miR-132* – microRNA 132; Pten – Phosphatase and Tensin homolog; *Akt* – proteine kinase B; *Foxo3* – *Forkhead box O3*; RT-PCR – Reverse transcription polymerase chain reaction; T2D – type 2 diabetes; BrdU – bromodeoxyuridine; LCM – laser capture microscopy; IPA – Ingenuity Pathway Analysis; *Pi3k* – Phosphatidylinositol-4,5-bisphosphate 3-kinase; *Ras* – Rat sarcoma; *Raf* – rapidly accelerated fibrosarcoma; *Mapk* – mitogen-activated protein kinase; *Sos1* – Son of sevenless homolog 1; *Gnb1* – G Protein Subunit Beta 1; *Nras* – Neuroblastoma RAS viral oncogene homolog; *Pik3r1* – Phosphoinositide-3- Kinase Regulatory Subunit 1; *Gnb* – G Protein Subunit Beta; *Fgfr3* – *fibroblast growth factor receptor 3; Creb* – cAMP response element-binding protein

Abstract

Aim and hypothesis:

microRNAs (miRNAs) play an integral role in maintaining beta cell function and identity. Deciphering their targets and precise role, however, remains a challenge. In this study we aimed to identify miRNAs and their downstream targets involved in regeneration of islet beta cells following partial pancreatectomy in mice.

Methods:

RNA from laser capture microdissected (LCM) islets of partially pancreatectomized and sham-operated mice were profiled with microarrays to identify putative miRNAs implicated in control of beta cell regeneration. Altered expression of selected miRNAs, including *miR-132*, was verified by RT-PCR. Potential targets of *miR-132* were selected through bioinformatic data mining. Predicted *miR-132* targets were validated for their changed RNA and protein expression levels and signaling upon *miR-132* knockdown or overexpression in MIN6 cells. The ability of *miR-132* to foster beta cell proliferation *in vivo* was further assessed in pancreatectomized *miR-132*$^{-/-}$ and control mice.

Results:

Partial pancreatectomy significantly increased the number of BrdU+/insulin+ positive islet cells. Microarray profiling revealed 14 miRNAs, including *miR-132* and *-141*, to be significantly upregulated in LCM islets of partially pancreatectomized compared to LCM islets of control mice. In the same comparison *miR-760* was the only miRNA found to be downregulated. Changed expression of these miRNAs in islets of partially pancreatectomized mice was confirmed by RT-PCR only in the case of *miR-132* and *-141*.

Based on previous knowledge of its function, we chose to focus our attention on *miR-132*. Downregulation of *miR-132* in MIN6 cells reduced proliferation while enhancing the expression of pro-apoptotic genes, which were instead reduced in *miR-132* overexpression MIN6 cells. Microarray profiling, RT-PCR and immunoblotting of *miR-132* overexpressing MIN6 cells revealed their downregulated expression of Pten, with concomitant increased levels of pro-proliferative factors phospho-Akt and phospho-Creb as well as inactivation of pro-apoptotic Foxo3 via its phosphorylation. Finally, we show that regeneration of beta cells following partial pancreatectomy was reduced in *miR-132*$^{-/-}$ mice compared to control mice.

Conclusions/Interpretations:

Our study provides compelling evidence for upregulation of *miR-132* being critical for regeneration of mouse islet beta cells *in vivo* through downregulation of its target Pten. Hence, the *miR-132*/Pten/Akt/Foxo3 signaling pathway may represent a suitable target to enhance beta cell mass.

Keywords

miR-132; beta cell function; beta cell regeneration; apoptosis; *Pten*; *Akt*; *Foxo3*; pancreatectomy, diabetes.

Research in Context

What is already known?

- Several miRNAs, including *miR-132*, are known to regulate beta cell function and mass in several mouse models of diabetes *db/db, ob/ob* and high fat-diet.

What is the key question?

- Which are the miRNAs implicated in control of beta cell regeneration upon partial pancreatectomy and how?

What are the new findings?

- *miR-132* is critical to promote regeneration of mouse beta cells *in vivo* following partial pancreatectomy
- In vitro studies in mouse MIN6 cells indicate that *miR-132* fosters beta cell proliferation by down-regulating the expression of phosphatase Pten, thereby tilting the balance between anti-apoptotic factor Akt and pro-apoptotic factor Foxo3 activities towards proliferation through regulation of their phosphorylation.

How might this impact on clinical practice in the foreseeable future?

- These findings strengthen the rationale for targeting the expression of *miR-132* to increase beta cell mass *in vivo* (type 2 diabetes) or *ex-vivo* (islet transplantation in type 1 diabetes) for the treatment of diabetes.

Introduction

miRNAs belong to the class of short non-coding RNAs that regulate gene expression by annealing to 3' untranslated region sequences in target mRNAs and inducing their post-transcriptional repression. The functional importance of miRNAs has been extensively investigated in recent years and their altered expression has been implicated in a wide range of diseases, including cancer [1], cardiovascular disease [2, 3] and diabetes [4]. In pancreatic beta cells, changed expression of miRNAs correlates with profound impairment of glucose metabolism [5] and processing of miRNAs appears to be altered in obesity, diabetes, and aging. Several miRNAs such as *miR-7*, *-21*, *-29*, *-34a*, *-132/-212*, *-184*, *-200* and *-375* have been found to be relevant for beta cell function [6]. RNA sequencing of human islets detected 346 miRNAs, including 40 which were enriched in comparison to other tissues [7]. *miR-375* is the most highly expressed miRNA in human and mouse pancreatic islets. Its down-regulation inhibits pancreatic islet development in *Xenopus laevis* [8], while its global inactivation in mice leads to decreased beta cell mass and ultimately diabetes [9, 10]. *miR-132* also plays a key role in beta cell function. Its expression is dysregulated in different mouse models of type 2 diabetes (T2D) [11-14], with its overexpression being correlated with improved glucose-stimulated insulin release from dissociated rat islet cells [13] as well as with enhanced beta cell proliferation and survival [12-14]. In primary PC12 cells, another endocrine cell model, *miR-132* controls cell survival by direct regulation of Pten, Foxo3a and p300 signaling [15]. However, in pancreatic islets, the functional relevance of *miR-132 in vivo* and its downstream targets remain unknown. To identify the major miRNAs as well as their downstream targets

involved in beta cell proliferation, we analyzed the profile of miRNAs differentially expressed after a partial pancreatectomy in comparison to sham-operated mice. We report here that the expression of 14 miRNAs were markedly increased and one miRNA was down-regulated in islets of partially pancreatectomized mice, in which beta cell proliferation was increased. Moreover, we show that down-regulation of *miR-132* expression in insulinoma MIN6 cells correlated with decreased proliferation and increased apoptosis by controlling the expression of *Pten* and its downstream effectors Akt and Foxo3 while its up-regulation had opposite effects, Finally we demonstrate that beta cell proliferation is impaired in *miR-132*$^{-/-}$ mice.

Methods

Mouse partial pancreatectomy

Mice underwent general anesthesia using a small rodents' anesthesia unit (Harvard Apparatus Ltd., Holliston, MA, USA) for mask inhalation of isoflurane (Baxter Deutschland GmbH, Unterschleißheim) at the concentration of 4.5–5% for induction and 2-2.5% for maintenance of anesthesia with an airflow rate of 200 ml/min. For perioperative analgesia buprenorphin (0.05 mg/kg bodyweight) was administered subcutaneously. The abdomen was opened through an upper midline incision. The spleen and the entire splenic portion of the pancreas were surgically removed while the mesenteric pancreas between the portal vein and the duodenum was left intact. The remnant was defined as the pancreatic tissue within 1-2 mm of the common bile duct that extends from the duct to the first portion of the duodenum. This remnant was the upper portion of the head of the pancreas. This procedure, as described previously [16] led to approximately 75% pancreatectomy, as confirmed by weighing the removed and remnant portions of the pancreas. Sham operations were performed by removing the spleen while leaving the pancreas intact. At the end of surgery, Alzet 1007D mini-osmotic pumps (Alzet®, Cupertino, CA, USA) were implanted i.p. to deliver 50 $\mu g \cdot \mu l^{-1}$ BrdU (Sigma, St. Louis, MO, USA) in 50% DMSO at a rate of 0.5 $\mu l \cdot h^{-1}$ for 7 days. Blood glucose levels were measured daily from the tail vein with a Glucotrend glucometer (Roche Diagnostics, Basel, Switzerland).

miR-132/-212$^{-/-}$ mice were backcrossed into the *C57Bl/6N* background for at least seven generations, as previously described [17]. Mutant and wild-type male *C57Bl/6N* mice with

an age of 13-19 weeks and a body weight of 28-34 g underwent partial pancreatectomy as described above. All animal protocols were approved by the institutional animal care and use committee at the Faculty of Medicine of TU Dresden and all experiments were performed in accordance with relevant guidelines and regulations.

Intraperitoneal glucose tolerance test (IpGTT)

IpGTT were performed two days before surgery and six days after surgery to assess differences between wild-type and mutant mice and between pancreatectomized and sham-operated animals. After 10 hours overnight fast, mice were injected with 2g/kg body weight of 20% glucose solution. Blood glucose levels were measured from the tail vein at 0, 15, 30, 60, 120 and 180 minutes after glucose injection.

BrdU staining of pancreatic tissue sections and MIN6 cells

The pancreatic remnants and the sham-operated pancreata were harvested 7 days post-surgery. Mice were anesthetized with isoflurane as described above and the abdominal incision was re-opened. After fixation by intracardial perfusion with 4% paraformaldehyde, mouse pancreas were removed, further fixed overnight in 10% neutral formalin, embedded in paraffin and cut in ten-micrometer thin serial sections. The core of the islets, containing predominantly beta cells, were obtained using laser capture microdissection (P.A.L.M. MicroBeam Laser Capture System, Zeiss Switzerland) after identifying islets on every fifth serial section by cresyl staining. The BrdU staining of pancreatic tissue sections and MIN6 cells was performed as previously described [16].

Transcriptomic profiling of mouse islets

Total RNA was isolated from the islets of 16-19-week-old wild-type and *miR-132*$^{-/-}$ mice (6 mice/group) using RNeasy (Qiagen, Hilden, Germany). For microarray analysis, 100 ng of islet RNA was amplified with the Illumina Total Prep RNA Amplification Kit (Ambion, Inc., Austin, TX, USA) and cRNA was labeled with biotin-UTP, as described [18].

Microarray analysis and data mining

Microarray data processing and quality control were done with GeneSpring GX 13. After quantile normalization, significantly differentially expressed genes were obtained by volcano plot filtering for FC≥|1.5| and $p<0.05$. Functional analysis was assessed using Ingenuity Pathway Analysis (IPA, Qiagen, Hilden, Germany).

Cloning of *miR-132* in *pacAd5* shuttle vector

To produce the adenovirus over-expressing *miR-132* we used the RAPAd® miRNA Adenoviral Expression System (Cellbiolabs, San Diego, CA, USA). Following the Kit's instructions, the mmu-*miR-132* precursor sequence, obtained from www.miRBase.org (*GGGCAACCGTGGCTTTCGATTGTTACTGTGGGAACCGGAGGTAACAGTCTACAGCC ATGGTCGCCC*), was PCR-amplified from mouse genomic DNA including approximately a 100bp flanking region on each side (Forward: *5'-TCGAGGATCCTCCCTGTGGGTTGCGG TGGG-3'*; Reverse: *5'-TCGAGCTAGCACATCGAATGTTGCGTCGCCGC-3'*) and cloned into the human β-globin Intron of the Kit's *pacAd5-miR-GFP-Puro* vector via *BamHI/NheI* digestion. This human β-globin intron, containing the mmu-*miR-132* precursor, was then

subcloned into the Kit's *pacAd5-CMV-eGFP* vector via PCR amplification (Forward: *5'-TGCAACCGGTGCCAGAACACAGGTACACATAT-3'*; Reverse:*5'-TGCAACCGGTCGTGC TTTGCCAAAGTGATG-3'*) and *AgeI* digestion to obtain a *miR-132* overexpressing schuttle vector with a CMV promoter. The empty *pacAd5-CMV-eGFP* vector was used for the production of a control virus.

Cell culture

Mouse MIN6 cells were kind gifts from Dr. Jun-ichi Miyazaki (Osaka University, Japan), and were grown as previously described [19]. MIN6 cells were cultured in 25 mmol/L glucose Dulbecco's modified Eagle's medium (DMEM, high glucose, GlutaMAX(TM), pyruvate) (Gibco, Thermo Fisher Scientific, Waltham, MA, USA), supplemented with 15% fetal bovine serum (Gibco, Thermo Fisher Scientific, Waltham, MA, USA), 100 U/mL penicillin, 100 U/mL streptomycin (Sigma-Aldrich, St. Louis, MO, USA) and 70μM β-Mercaptoethanol (Sigma-Aldrich, St. Louis, MO, USA), and were incubated at 37°C in a humidified atmosphere containing 95% air and 5% CO_2. HEK293T cells used to propagate the adenovirus were cultured in 25 mmol/L glucose Dulbecco's modified Eagle's medium (DMEM, high glucose, GlutaMAX(TM), pyruvate) (Gibco), supplemented with 10% fetal bovine serum (Gibco), 100 U/mL penicillin, 100 U/mL streptomycin (Sigma-Aldrich) and 0.1 mM non-essential amino acids (Gibco), and were incubated at 37°C in a humidified atmosphere containing 95% air and 5% CO_2.

Adenovirus production in HEK293T cells

The adenoviral backbone vector *pacAd5-9.2-100* from the RAPAd miRNA Adenoviral Expression System (Cellbiolabs, San Diego, CA, USA) and both shuttle vectors *pacAd5-CMV-eGFP* and *pacAd5-CMV-mir132-eGFP* were *PacI* linearized, and co-transfected into HEK293T cells using the X-tremeGENE 9 DNA Transfection Reagent (Roche, Basel, Switzerland) and amplified, until a sufficient amount of virus supernatant was available for experiments, which was then aliquoted and stored at -80°C. Virus titers were determined with the Adeno-X^{TM} Rapid Titer Kit (Clontech, Mountain View, CA, USA) All steps were carried out according to the manufacturer's instructions.

Alteration of *miR-132* expression in MIN6 cells with siRNAs or adenoviruses

The single-stranded RNA used in to silence *miR-132* consisted of 24-nucleotide length oligo: *5'-CGACCAUGGCUGUAGACUGUUACC-3'* and as control, we used a scrambled oligonucleotide. MIN6 cells were seeded in a 6-well plate as described above on day 1. For the silencing of *miR-132*, cells were transfected with 100 nM of anti-*miR-132* or control siRNAs using Dharmafect4 as transfection reagent on day 2. For the overexpression of *miR-132*, MIN6 cells were transduced with an adenovirus in which *miR-132* was driven by the CMV promoter at MOI of 6,400. On day 4 post RNA silencing or adenoviral transduction, cells were harvested, proceeded for BrdU labeling or western blotting as described below.

Cell extraction and immunoblotting

MIN6 cells were harvested at 4°C in RIPA buffer [50 mM Tris·HCl, pH 8.0, 150 mM NaCl, 1% Nonidet P-40, 0.1% SDS, 0.5% sodium deoxycholate, and protease inhibitor mixture (Sigma)] for total protein extraction. Insoluble material was removed by centrifugation. Aliquots of 20 ug were separated by SDS PAGE, as described ([16]. The source, species and dilutions of antibodies used for immunoblotting are listed in ESM Table 1.

RNA Isolation from MIN6 Cells for microRNA measurement

Cells were harvested after washing them once in Dulbecco's PBS (Sigma, St. Louis, MO, USA) by scraping and pelleting them 5 min at 300 x g at 4°C. Cell pellets were immediately stored at -80°C. miRNA isolation was performed with the mirVana miRNA Isolation Kit (Ambion, Foster City, CA, USA) according to the manufacturer's instructions. Both, the total RNA and the microRNA-enriched fraction were isolated. RNA concentrations were measured at the Nanodrop ND-1000 Spectrophotometer (PEQLAB / VWR, Darmstadt, Germany). Samples were stored at -80°C.

Taqman microRNA Assay

Reverse transcription of 15 ng miRNA per reaction of the miRNA-enriched fraction into cDNA was performed with the TaqMan® MicroRNA Reverse Transcription Kit (Applied Biosystems) using the mir-132-specific or the U6 snRNA-specific stem-looped RT-Primer of the Taqman® Micro RNA Assay hsa-miR-132 (Applied Biosystems, Cat.# 4427975, Assay# 000457 / Thermo Fisher Scientific, Waldham, MA, USA) or the Taqman® Micro RNA Control Assay U6 snRNA (Applied Biosystems, Cat.# 4427975, Assay# 001973 /

Thermo Fisher Scientific, Waldham, MA, USA). Both transcriptions were performed from each sample. Real time-PCR was then performed with the TaqMan® Universal PCR Master Mix (Applied Biosystems / Thermo Fisher Scientific, Waldham, MA, USA) on the Aria MX Real-Time PCR System (Agilent Technologies) using the small RNA-specific Primer mixes of the TaqMan® Assays described above. All steps were carried out according to the manufacturer's instructions.

Real Time-PCR

cDNA samples were obtained by reverse transcription of 1ug total RNA using the M-MLV Reverse Transcriptase (Promega, USA, WI, Madison). Quantitative real time-PCR was then performed with the GoTaq qPCR Master Mix (Promega, USA, WI, Madison) according to the manufacturers instruction using the oligonucleotides listed in ESM Table 2.

Statistical analysis

Statistical analyses were performed by using the unpaired Student's *t* test unless otherwise stated. Results are presented as mean SE unless otherwise stated. A value of $p < 0.05$ was considered significant. Error bars show standard deviations from at least three independent experiments unless otherwise stated. Histograms were prepared with Microsoft Excel (Microsoft, Redmont, WA, USA) or GraphPad Prism.

Results

miR-132 is upregulated in proliferating islet cells of pancreatectomized mice

To identify key miRNAs involved in beta cell proliferation, we used partially pancreatectomized mice (n=3) as a model for beta cell regeneration (Fig. 1a). The removal of 70-80% of the pancreas is a well-established procedure for inducing the replication of beta cells in the remaining pancreas [16, 20]. Proliferating cells were stained with 25µg/hr BrdU continuously delivered by an osmotic mini-pump implanted in the abdomen at the time of pancreatectomy. This approach ensures the labeling of every dividing cell [16]. As controls, 4 mice were similarly implanted with an osmotic mini-pump for BrdU delivery, but only underwent total splenectomy. Seven days post-surgery, all mice were sacrificed, their remnant pancreas excised for serial sectioning (40 sections/mouse) and staining with cresyl-violet to locate the islets. Adjacent, unstained sections were then used to count $BrdU^+$ cells in the islet cores, which in rodents consists mainly of beta cells [21] (Fig. 1b) prior to islet core excision by laser capture microdissection (LCM) (Fig. 1 a and b). As expected, in partially pancreatectomized mice the fraction of islet core $BrdU^+$ cells/total islet core cells, as determined by nuclear counting, was significantly higher than in sham-operated mice (Fig. 1c). RNA extracted from LCM islet cores was then profiled using microarrays. Fourteen miRNAs were found to be differently expressed (cut-off values: p= 0.05; FC≥1.5) in the islet cores of partially pancreatectomized mice compared to sham operated mice (Table 1). All these miRNAs were up-regulated, except *miR-760*, which was reduced by 2.28 fold. Expression levels of all 14 differentially expressed miRNAs were further quantified by real-time PCR (RT-PCR). With this analysis, only the significant

changed expression of *miR-132* and *miR-141* could be validated (ESM Table 3). Given the role of *miR-132* in the cell replication *in vitro* of primary islet cells [13], and other cell types, including glioma cells [22] and epidermal keratinocytes [23], we focus our attention on the potential involvement and mode of action of this miRNA in the regulation of beta cell proliferation.

miR-132 **promotes proliferation and survival of mouse insulinoma MIN6 cells**

At first, we down-regulated *miR-132* expression in mouse insulinoma MIN6 cells using an anti-microRNA approach. Reduced expression of *miR-132* by 90% (n=3, Fig. 2a), as assessed by RT-PCR, correlated with a slight, but significant reduction in the percentage of $BrdU^+$ MIN6 cells in comparison to cells [n=6, 24.48$\pm$1.78 % (6,088 $BrdU^+$ out of 25,246 cells) vs. 27.35$\pm$2.23% (7,271 $BrdU^+$ cells out of 27,413 cells), p-value= 0.039], which had been transfected with a control oligonucleotide (Fig. 2b-d). *miR-132* depletion correlated also with increased detection of cleaved Caspase-9 (n= 6; Fig. 2e and f), while the levels of cleaved Caspase-3 were not significantly changed. Conversely, overexpression of *miR-132* with a bi-cistronic adenovirus vector encoding also for eGFP (n= 3 Fig. 2g) was not associated with a further increase in the proliferation of MIN6 cells, presumably due to their neoplastic state (n= 3, Fig. 2h-j). However, overexpression of *miR-132* correlated with reduced levels of pro- and cleaved Caspase-9 (n= 6, Fig. 2k and l), consistent with *miR-132* being anti-apoptotic.

miR-132 regulates the expression of *Pten* and *Mapk1* in MIN6 cells

Next, we aimed to uncover down-stream targets of *miR-132* in MIN6 cells. Microarray gene expression analysis of *miR-132* overexpressing MIN6 cells identified 345 unique differentially expressed genes (cut-off values: $p<0.05$, FC ≥1.5), with 194 (56.2%) being down regulated and 151 (43.8%) up-regulated (Fig. 3a and ESM Table 4). Querying the TargetScan Mouse 7.1 database 35 of the down- and 2 of the up-regulated genes were predicted to contain highly conserved binding sites for *miR-132* (Fig. 3a and ESM Table 5). Further analysis of regulated genes with Ingenuity Pathway Analysis revealed 8 regulated pathways (Fig. 3b and ESM Table 6), which included 26 of the 345 differentially expressed genes, all related to cell proliferation and survival (Fig. 3c). Among these 26 genes, the top 10 most represented genes in the 8 signaling pathways were further selected for validation of their mRNA levels by RT-PCR (ESM Table 7). As control, we also assessed the mRNA expression levels of *Rasa1*, an established target of *miR-132* [24]. As shown in Fig. 3d, 6 out of 10 of the selected genes, namely *Mapk1/Erk2*, *Pten*, *Nras*, *Pik3r1*, *Gnb1* and *Gnb5* were confirmed to be downregulated upon *miR-132* overexpression. Three of them, *Mapk1, Pten* and *Gnb1,* were also among the 37 predicted targets for *miR-132* binding (ESM Table 5). Notably, *Mapk1,* also known as *Erk2,* is a serine-threonine kinase located downstream of the tumor-suppressor phosphatase *Pten* and both genes play a critical role in control of cell proliferation and survival [25, 26].

miR-132 regulates *Pten* signaling in MIN6 cells

Next, we tested whether overexpression of *miR-132* affected the protein levels of the Pten and Mapk1/Erk2. Immunoblotting of MIN6 cells transduced with the *miR-132*/*eGFP* viral

vector confirmed the down-regulation of Pten in parallel with up-regulation of its targets Akt and phospho-Akt (S473) (Fig. 4a and b), while *Akt* mRNA levels were unchanged (ESM Fig. 1). Furthermore, levels of the Akt1 substrate Creb and phospho-Creb (S133) were unchanged, but the phospho-Creb/Creb ratio was also increased. Likewise, overexpression of *miR-132* correlated with reduced expression of Mapk1/Erk2, phospho-Mapk1/Erk2 and Rasa1/RasGAP, but not of Erk1 and phospho-Erk1 (Fig. 4c and d).

As down-regulation of *miR-132* correlated with elevated cleaved Caspase-9 levels, we further tested whether its overexpression affected the expression of *Foxo3a,* a key mediator of apoptosis. Immunoblotting for Foxo3a showed that its phosphorylation, which inhibits its activity, was increased (Fig. 4e-f), although the overall levels of its mRNA (ESM Fig. 1) and protein (Fig. 4e-f) were not changed.

miR-132 **deletion impairs islet beta cell proliferation in pancreatectomized mice**

Finally, to verify that *miR-132* positively affects beta cell regeneration *in vivo*, we investigated beta cell proliferation in partially pancreatectomized or sham operated *miR-132*$^{-/-}$ mice and control littermates (6 mice/group), as described previously [16]. Intraperitoneal glucose tolerance test prior and 6 days after surgery showed no difference between control and *miR-132*$^{-/-}$ mice (Fig. 5a and b). Daily blood glucose measurements, in particular, showed a comparable slight decrease of glycaemia in partially pancreatectomized wild-type and *miR-132*$^{-/-}$ mice relative to sham operated mice in the first day post-surgery, followed by a complete normalization of glycaemia by the end of the 1-week-long protocol (ESM Fig. 2). Seven days after surgery, the mice were sacrificed, the remnant pancreas excised, and BrdU^{+}/insulin^{+} beta cells were counted (Fig. 5c-f and ESM

Table 8). As assessed by immunostaining for insulin, the average number of beta cells/islet in wt (31,9 beta cells/islet) and *miR-132*$^{-/-}$ (31,7 beta cells/islet) was increased in partially pancreatectomized mice relative to their sham-operated counterparts (wt: 23,8 beta cells/islet; *miR-132*$^{-/-}$: 26,8 beta cells/islet). Likewise, the number BrdU^{+} insulin^{+} beta cells was increased in both groups of partially pancreatectomized mice compared to sham operated mice (Fig. 5g, ESM Table 8). However, in partially pancreatectomized *miR-132*$^{-/-}$ mice there were fewer BrdU^{+}/insulin^{+} cells than in partially pancreatectomized wt mice (Fig. 5g, ESM Table 8). These data provide conclusive evidence for *miR-132* exerting a positive role for beta cell regeneration *in-vivo*.

Discussion

miR-132 is known *to* control many cellular processes in various tissues including neuronal morphogenesis and regulation of circadian rhythm. *miR-132* altered expression correlated with several neurological disorders, such as Alzheimer's and Huntington's diseases [15, 27] Thus, most of our acknowledge about *miR-132* regulation and biological functions emerged from studies performed on neural cells, while not much is already known about the downstream target of *miR-132* in pancreatic beta cells. *miR-132* and *miR-212* have identical seed sequences and potentially have targets in common. Here we have identified *miR-132* as one of the mostly up-regulated miRNAs with a 5-fold expression change in pancreatectomized mice, a condition known to induce beta cell proliferation. This finding is in agreement with previous data showing induced *miR-132* expression in different models of type 2 diabetes, including *db/db*, high-fat diet-fed [13] and *ob/ob* mice [10, 28]. Among our list of differentially expressed miRNAs in islets of partially pancreatectomized mice, *miR-205* showed the greatest change (5 fold). Interestingly, *miR-205* has also been described to be the miRNA with the highest expression change in hepatocytes of mice with obesity-induced type 2 diabetes [28]. On the other hand, our analysis did not reveal a significant change in the expression of *miR-375*, a miRNA abundant in pancreatic islets known to regulate insulin secretion and beta cell proliferation [10].

Previous work has shown that *miR-132* is highly expressed in neurons and may regulate their differentiation [29, 30]. More recent work on primary neurons and PC12 cells has shown that *miR-132* controls cell survival by direct regulation of Pten, Foxo3a and p300 - ,

proteins involved in Alzheimer's disease [15]. To uncover the down stream target of *miR-132* in beta cells, we first investigated whether *miR-132* has a proliferative role in insulinoma MIN6 cells. We found that *miR-132* down-regulation with anti-*miR-132* correlated with slight but significant inhibition of MIN6 cells proliferation. The inhibition of the expression of *miR-132* showed also an increase in cleaved Caspase-9-mediated apoptosis. Conversely, its up-regulation has a protective effect by reducing Caspase-9 processing. However, the increase in the expression of *miR-132* did not correlate with an enhancement in the proliferative rate of MIN6 cells, presumably due to their higher proliferative fate. To uncover the downstream targets of *miR-132*, we analyzed the expression pattern of differentially expressed genes in cells over-expressing *miR-132*. *Pten* expression which is known to inversely correlate with cell survival, was significantly down-regulated in agreement with our data showing decreased apoptosis upon overexpression of *miR-132*. The reduced expression of *Pten* upon overexpression of *miR-132* was confirmed at the protein level. Importantly, reduction of Pten correlated with increased phosphorylation of Akt (P-Akt) and Foxo3. P-Akt is a major activator of Foxo family proteins, which are members of the Forkhead superfamily of winged helix transcription factors controlling cellular metabolism, stress responses, DNA damage repair and cell death. P-Foxo3 can be phosphorylated on Thr32, Ser253 and Ser315 which promotes its and association with 14-3-3 proteins for retention in the cytoplasm, and thereby inhibition of its transcriptional activity [31].

Mapk1/Erk2 (mitogen-activated protein kinase 1) expression is reduced in cells over-expressing *miR-132* and survey of Erk2 activation reveals reduced phosphorylation of

Erk2 without change in its activation state (as shown by the ratio of p-Erk2/Erk2) suggesting that the Ras/Raf/Erk1/2 pathway is not preponderant in this biological process.

A considerable number of miRNAs have been associated with pancreatic beta cell development by affecting proliferation or differentiation (e.g., *miR-375* [10], *miR-7* [32], *miR-124a* [33], *miR-24* [34], *let-7a* [31], *miR-26a* [35], *miR-184* [14], *miR-195*, *miR-15*, *miR-16* [37] and *miR-132* [13, 28]. Among those miRNAs, *miR-132* was consistently differentially expressed in various T2D models in which beta cells were challenged by increased metabolic demand, condition known to promote beta cell proliferation, including obesity induced diabetes [28]. In mouse model, constitutive deletion of *miR-132* resulted in mice with deficient endocrine development [17]. A specific deletion of *miR-13*/*212* locus in adult hippocampus with a retrovirus expressing Cre recombinase caused a dramatic decrease in dendrite length, arborization and spine density, suggesting that *miR-132*/*212* is required for normal dendritic maturation in adult hippocampal neurons [38]. Here we demonstrate that regeneration of beta cells in pancreatectomized *miR-132*$^{-/-}$ mice is reduced, conceivably through its control of the Pten/Pi3K/Akt signaling.

In conclusion, we have identified *miR-132* as a critical epigenetic factor for replication of beta cell after injury, such as partial pancreatectomy, and shed light about its mechanism of action in beta cells. Targeted therapies for beta cell regeneration in type 1 and type 2 diabetes are actively sought, and in this context *miR-132* appears to be a worthy candidate to be considered. Along these lines, it would be especially interesting in the future to determine which and how extracellular signals promotes its expression in beta cells.

Acknowledgements

We are grateful to Julia Jarrells in the Sequencing Facility at the Max Planck Institute for Molecular Cell Biology and Genetics, Dresden, Germany; Anke Sönmez (Dresden, Germany) for help with cell culture, Katja Pfriem (Dresden, Germany) for administrative assistance and all the colleagues in the Department of General, Thoracic and Vascular Surgery in the Faculty of Medicine at TU Dresden for their support.

Data availability

Original microarray data will be accessible through the GEO database (https://www.ncbi.nlm.nih.gov/geo/).

Funding

This study was partially supported with funds from the German Center for Diabetes Research (DZD e.V.) by the German Ministry for Education and Research to MS and SK; and by a MeDDrive grant from the Carl Gustav Carus Faculty of Medicine at TU Dresden to SW.

Duality of interest statement

The authors do not have duality of interest associated with this manuscript.

Contribution statement

HM, MS and SK conceived the study and the experimental design; GH profiled gene expression, performed the data mining and validated the target genes with the help of KG,

JM, KPK and SW; SH and JM performed the pancreatectomy, implanted the BrdU pump and immunostained pancreatic islets under the supervision of SK. KC generated and provided the *miR-132*$^{-/-}$ mice. HM, MS and SK wrote the manuscript. HM, MS and SK are responsible for the integrity of the study.

Figure and Table Legends

Figure 1. ***miR-132* expression is induced in pancreatectomized mice**

(**a**) Overview of the experimental design. (**b**) A tissue section of the remnant pancreas 1-week after partial pancreatectomy stained with cresyl-violet to reveal the islet core, and labeled with DAPI (green) and anti-BrdU antibodies (black) to detect cell nuclei and replicating cells, respectively. (**c**) Percentage of $BrdU^+$ cells in islet cores. The analysis included 7 mice, of which 4 were shamp operated and 3 were partially pancreatectomized. 40 slices/group were counted for $BrdU^+$ cells. *, $p < 0.05$.

Figure 2. *miR-132* regulates the proliferation and cell survival in MIN6 cells

(**a**) Levels of *miR-132* in MIN6 cells treated with control (white bar) or *miR-132* (black bar) siRNA, as determined by RT-PCR. (**b-c**) Representative confocal images of $BrdU^+$ cells (red) in MIN6 cells treated with control (**b**) or *miR-132* (**c**) siRNA. (**d**) Number of total (white bars) and $BrdU^+$ (black bars) MIN6 cells counted from images as in (**b-c**). (**e**) Representative immunoblots for pro- and cleaved caspase-9, cleaved caspase-3 and γ-tubulin as loading control in extracts of MIN6 cells treated with control or *miR-132* siRNA. (**f**) Densitometric quantification of immunoblots as in (**e**). White bars: control siRNA treated cells; black bars: *miR-132* siRNA treated cells. (**g**) Expression levels of *miR-132* in MIN6 cells transduced with adenovirus vectors for co-expression of *miR-132* and *eGFP* (black bar) or *eGFP* alone (white bar), as detected by RT-PCR. (**h-i**) Representative confocal images of $BrdU^+$ (red), and $eGFP^+$ (green) MIN6 cells transduced with adenovirus vectors for co-expression of *miR-132* and *eGFP* (**i**) or *eGFP* alone. Nuclei were detected with

DAPI (blue). (**h**) Number of total (white bars) and $BrdU^+$ (black bars) MIN6 cells counted from images as in (**h-i**). (**k**) Representative immunoblots for pro- and cleaved caspase-9, cleaved caspase-3 and γ-tubulin as loading control in extracts of MIN6 cells transduced with adenovirus vectors for co-expression of *miR-132* and *eGFP* or *eGFP* alone. (**l**) Densitometric quantification of immunoblots as in (**k**). White bars: cells transduced with *CMV-eGFP* adenovirus vector; black bars: cells transduced with *CMV-miR-132-eGFP* adenovirus vector. Data shown in (**a**), (**g**) and (**j**) are from 3 independent experiments, while those shown in (**d**), (**f**) and (**l**) are from 6 independent experiments. Scale bars in (**b-c**) and (**h-i**)= 50µm. * $p < 0.05$, **<0.01, **<0.001.

Figure 3. Identification and validation of *miR-132* target genes in MIN6 cells

(**a**) Venn diagram showing the number of down- and up-regulated genes in MIN6 cells transduced with *CMV-miR-132/eGFP* adenovirus vector compared to MIN6 cells transduced with *CMV-eGFP* adenovirus vector and their overlap with predicted highly conserved *murine mouse* targets of *miR-132.* (**b**) Ingenuity Pathway Analysis of significantly altered pathways in MIN6 cells overexpressing *miR-132* and *eGFP* compared to MIN6 cells overexpressing *eGFP* alone. (**c**) Heat-map of the 26 (red vertical bar: cluster of down-regulated genes; blue vertical bar: cluster of up-regulated genes) among the 345 differentially expressed genes included in the 8 regulated pathways indicated in (**b**) and related to cell proliferation and survival in MIN6 cells overexpressing *miR-132* and *eGFP* relative to MIN6 cells overexpressing *eGFP* alone. Brightest shades of yellow and blue reflect the higher and lower expression levels of a given gene, as indicated in top horizontal bar. The results are from 3 independent microarray analyses. (**d**) Validation by

RT-PCR of the expression levels of the top 10 most represented genes in the 8 signaling pathways shown in (**b**) and among the 26 regulated genes shown in (**c**). White bars: expression in MIN6 cells overexpressing *eGFP* alone; black bars: expression in MIN6 cells overexpressing *miR-132* and *eGFP.* * $p < 0.05$, **<0.01, **<0.001. In (**b**) significance was assessed using the Benjamini-Hochberg test.

Figure 4. Validation of gene profiling data in MIN6 Cells overexpressing miR132

(**a, c, e**) Representative immunoblots for the indicated proteins on cell extracts of MIN6 cells overexpressing *miR-132* and *eGFP* or *eGFP* alone. (**b, d and f**) Densitometric quantification of the indicated proteins, as detected by immunblots in (**a**), (**c**) and (**e**), respectively. Data are from 6 independent experiments. * $p < 0.05$, **<0.01, **<0.001.

Figure 5. Impaired pancreatic beta cells regeneration in *miR-132*$^{-/-}$ mice

(**a)** Excursion of blood glucose levels in wild-type (green line) and *miR-132*$^{-/-}$ (red line) mice during an intraperitoneal glucose tolerance test performed two days before surgery. (**b**) Excursion of blood glucose levels in wild-type and *miR-132*$^{-/-}$ partially pancreatectomized or sham-operated mice during an intraperitoneal glucose tolerance test performed six days after surgery. Sham-operated wild-type mice: blue line; partially pancreatectomized wild-type mice: green line; sham-operated *miR-132*$^{-/-}$ mice: red line; partially pancreatectomized *miR-132*$^{-/-}$ mice: purple line. (**c**-**f**) Representative confocal images of paraffin pancreatic sections from wild-type sham-operated (**c**) or partially pancreatectomized mice (**e**) or from *miR-132*$^{-/-}$ sham-operated (**d**) or partially pancreatectomized (**f**) mice. Sections were immunolabeled for insulin (red) and BrdU

(green), while nuclei were detected with DAPI (blue). (**g**) Percentage of $BrdU^+$, $insulin^+$ cells. White bars: wild-type mice; black bars: *miR-132*$^{-/-}$ mice. Data are from 3 independent series with two mice for each group. Up to 50 islets were counted for each mouse for a total of 250-300 islets per group. *, $p < 0.05$.

Table 1. Differentially expressed miRNAs in islet cores of partially pancreatectomized mice. miRNA are ranked by fold change (absolute value).

References

[1] Li Y, Zu L, Wang Y, Wang M, Chen P, Zhou Q (2015) miR-132 inhibits lung cancer cell migration and invasion by targeting SOX4. Journal of thoracic disease 7: 1563-1569

[2] Gupta MK, Halley C, Duan ZH, et al. (2013) miRNA-548c: a specific signature in circulating PBMCs from dilated cardiomyopathy patients. Journal of molecular and cellular cardiology 62: 131-141

[3] Huang ZP, Chen J, Seok HY, et al. (2013) MicroRNA-22 regulates cardiac hypertrophy and remodeling in response to stress. Circulation research 112: 1234-1243

[4] Guay C, Regazzi R (2015) Role of islet microRNAs in diabetes: which model for which question? Diabetologia 58: 456-463

[5] Dey N, Das F, Mariappan MM, et al. (2011) MicroRNA-21 orchestrates high glucose-induced signals to TOR complex 1, resulting in renal cell pathology in diabetes. The Journal of biological chemistry 286: 25586-25603

[6] Dalgaard LT, Eliasson L (2017) An 'alpha-beta' of pancreatic islet microribonucleotides. The international journal of biochemistry & cell biology

[7] van de Bunt M, Gaulton KJ, Parts L, et al. (2013) The miRNA profile of human pancreatic islets and beta-cells and relationship to type 2 diabetes pathogenesis. PloS one 8: e55272

[8] Kloosterman WP, Lagendijk AK, Ketting RF, Moulton JD, Plasterk RH (2007) Targeted inhibition of miRNA maturation with morpholinos reveals a role for miR-375 in pancreatic islet development. PLoS biology 5: e203

[9] Latreille M, Herrmanns K, Renwick N, et al. (2015) miR-375 gene dosage in pancreatic beta-cells: implications for regulation of beta-cell mass and biomarker development. Journal of molecular medicine 93: 1159-1169

[10] Poy MN, Hausser J, Trajkovski M, et al. (2009) miR-375 maintains normal pancreatic alpha- and beta-cell mass. Proceedings of the National Academy of Sciences of the United States of America 106: 5813-5818

[11] Esguerra JL, Bolmeson C, Cilio CM, Eliasson L (2011) Differential glucose-regulation of microRNAs in pancreatic islets of non-obese type 2 diabetes model Goto-Kakizaki rat. PloS one 6: e18613

[12] Jacovetti C, Abderrahmani A, Parnaud G, et al. (2012) MicroRNAs contribute to compensatory beta cell expansion during pregnancy and obesity. The Journal of clinical investigation 122: 3541-3551

[13] Nesca V, Guay C, Jacovetti C, et al. (2013) Identification of particular groups of microRNAs that positively or negatively impact on beta cell function in obese models of type 2 diabetes. Diabetologia 56: 2203-2212

[14] Tattikota SG, Rathjen T, McAnulty SJ, et al. (2014) Argonaute2 mediates compensatory expansion of the pancreatic beta cell. Cell metabolism 19: 122-134

[15] Wong HK, Veremeyko T, Patel N, et al. (2013) De-repression of FOXO3a death axis by microRNA-132 and -212 causes neuronal apoptosis in Alzheimer's disease. Human molecular genetics 22: 3077-3092

[16] Mziaut H, Kersting S, Knoch KP, et al. (2008) ICA512 signaling enhances pancreatic beta-cell proliferation by regulating cyclins D through STATs. Proceedings of the National Academy of Sciences of the United States of America 105: 674-679

[17] Ucar A, Vafaizadeh V, Jarry H, et al. (2010) miR-212 and miR-132 are required for epithelial stromal interactions necessary for mouse mammary gland development. Nature genetics 42: 1101-1108

[18] Mziaut H, Mulligan B, Hoboth P, et al. (2016) The F-actin modifier villin regulates insulin granule dynamics and exocytosis downstream of islet cell autoantigen 512. Molecular metabolism 5: 656-668

[19] Miyazaki J, Araki K, Yamato E, et al. (1990) Establishment of a pancreatic beta cell line that retains glucose-inducible insulin secretion: special reference to expression of glucose transporter isoforms. Endocrinology 127: 126-132

[20] Bonner-Weir S, Baxter LA, Schuppin GT, Smith FE (1993) A second pathway for regeneration of adult exocrine and endocrine pancreas. A possible recapitulation of embryonic development. Diabetes 42: 1715-1720

[21] Elayat AA, el-Naggar MM, Tahir M. (1995). An immunocytochemical and morphometric study of the rat pancreatic islets. J Anat.186:629–37

[22] Chen S, Wang Y, Ni C, Meng G, Sheng X (2016) HLF/miR-132/TTK axis regulates cell proliferation, metastasis and radiosensitivity of glioma cells. Biomedicine & pharmacotherapy = Biomedecine & pharmacotherapie 83: 898-904

[23] Li D, Wang A, Liu X, et al. (2015) MicroRNA-132 enhances transition from inflammation to proliferation during wound healing. The Journal of clinical investigation 125: 3008-3026

[24] Anand S, Majeti BK, Acevedo LM, et al. (2010) MicroRNA-132-mediated loss of p120RasGAP activates the endothelium to facilitate pathological angiogenesis. Nature medicine 16: 909-914

[25] Deb TB, Barndt RJ, Zuo AH, Sengupta S, Coticchia CM, Johnson MD (2014) PTEN-mediated ERK1/2 inhibition and paradoxical cellular proliferation following Pnck overexpression. Cell cycle 13: 961-973

[26] Huang YC, Yu HS, Chai CY (2015) Roles of oxidative stress and the ERK1/2, PTEN and p70S6K signaling pathways in arsenite-induced autophagy. Toxicology letters 239: 172-181

[27] Lee ST, Chu K, Im WS, et al. (2011) Altered microRNA regulation in Huntington's disease models. Experimental neurology 227: 172-179

[28] Zhao E, Keller MP, Rabaglia ME, et al. (2009) Obesity and genetics regulate microRNAs in islets, liver, and adipose of diabetic mice. Mammalian genome : official journal of the International Mammalian Genome Society 20: 476-485

[29] Vo N, Klein ME, Varlamova O, et al. (2005) A cAMP-response element binding protein-induced microRNA regulates neuronal morphogenesis. Proceedings of the National Academy of Sciences of the United States of America 102: 16426-16431

[30] Wayman GA, Davare M, Ando H, et al. (2008) An activity-regulated microRNA controls dendritic plasticity by down-regulating p250GAP. Proceedings of the National Academy of Sciences of the United States of America 105: 9093-9098

[31] Brunet A, Bonni A, Zigmond MJ, et al. (1999). Akt promotes cell survival by phosphorylating and inhibiting a Forkhead transcription factor. Cell. 96: 857-868

[32] Wang Y, Liu J, Liu C, Naji A, Stoffers DA. (2013). MicroRNA-7 regulates the mTOR pathway and proliferation in adult pancreaticβ-cells. Diabetes. 62:887-95

[33] Baroukh N, Ravier MA, Loder MK, et al. (2007) MicroRNA-124a regulates Foxa2 expression and intracellular signaling in pancreatic beta-cell lines. The Journal of biological chemistry 282: 19575-19588

[34] Vijayaraghavan J, Maggi EC, Crabtree JS (2014) miR-24 regulates menin in the endocrine pancreas. American journal of physiology Endocrinology and metabolism 307: E84-92

[35] Gurung B, Muhammad AB, Hua X (2014) Menin is required for optimal processing of the microRNA let-7a. The Journal of biological chemistry 289: 9902-9908

[36] Fu X, Jin L, Wang X, et al. (2013) MicroRNA-26a targets ten eleven translocation enzymes and is regulated during pancreatic cell differentiation. Proceedings of the National Academy of Sciences of the United States of America 110: 17892-17897

[37] Joglekar MV, Parekh VS, Mehta S, Bhonde RR, Hardikar AA (2007) MicroRNA profiling of developing and regenerating pancreas reveal post-transcriptional regulation of neurogenin3. Developmental biology 311: 603-612

[38] Magill ST, Cambronne XA, Luikart BW, et al. (2010) microRNA-132 regulates dendritic growth and arborization of newborn neurons in the adult hippocampus. Proceedings of the National Academy of Sciences of the United States of America 107: 20382-20387.

Figure 1

a

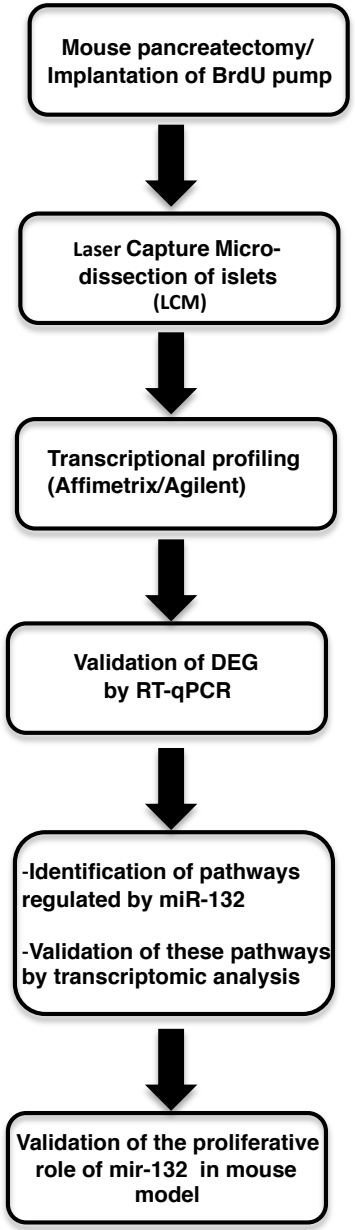
Mouse pancreatectomy/
Implantation of BrdU pump
Laser Capture Micro-
dissection of islets
(LCM)
Transcriptional profiling
(Affimetrix/Agilent)
Validation of DEG
by RT-qPCR
-Identification of pathways
regulated by miR-132
-Validation of these pathways
by transcriptomic analysis
Validation of the proliferative
role of mir-132 in mouse
model

b

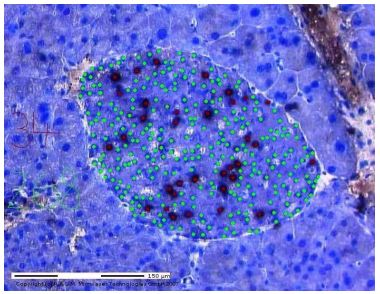

c

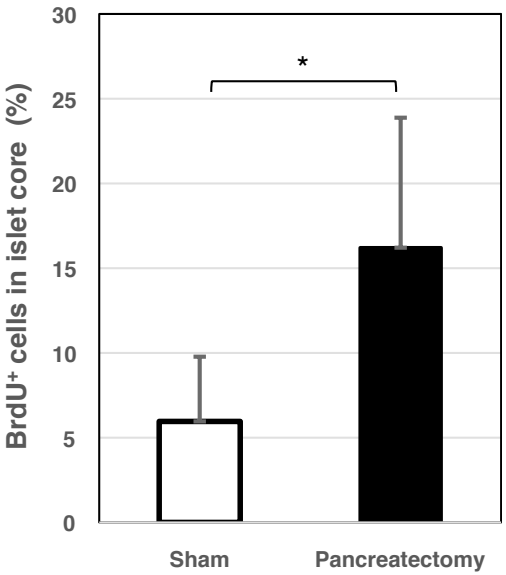
30
25
20
15
10
5
0
*
BrdU+ cells in islet core (%)
Sham
Pancreatectomy

Figure 2

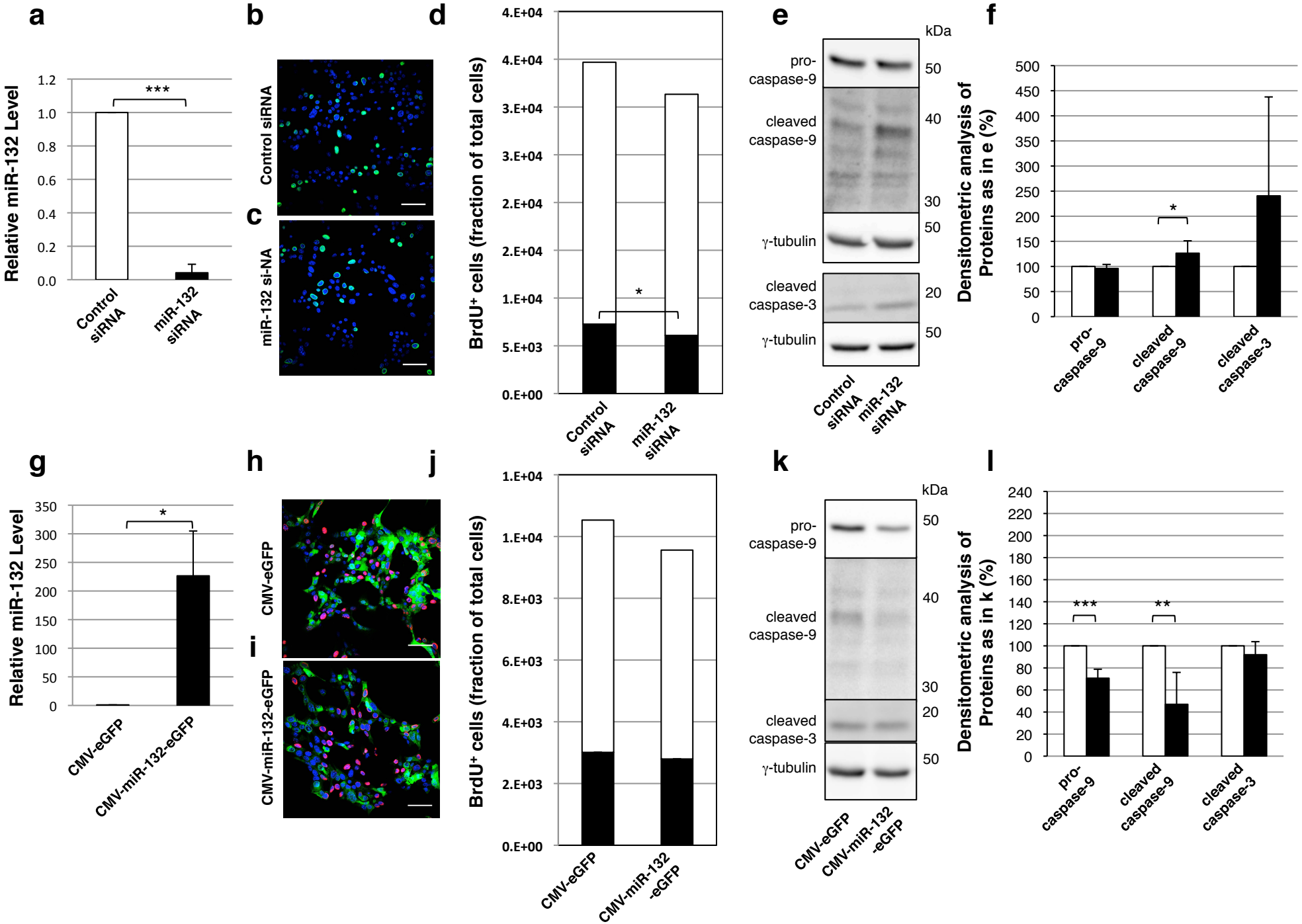
a
Relative miR-132 Level
1.2
1.0
0.8
0.6
0.4
0.2
0.0
***
Control siRNA
miR-132 siRNA
b
Control siRNA
c
miR-132 si-NA
d
BrdU+ cells (fraction of total cells)
4.E+04
4.E+04
3.E+04
3.E+04
2.E+04
2.E+04
1.E+04
5.E+03
0.E+00
*
Control siRNA
miR-132 siRNA
e
kDa
pro-caspase-9
cleaved caspase-9
γ-tubulin
cleaved caspase-3
γ-tubulin
50
40
30
50
20
50
Control siRNA
miR-132 siRNA
f
Densitometric analysis of Proteins as in e (%)
500
450
400
350
300
250
200
150
100
50
0
*
pro-caspase-9
cleaved caspase-9
cleaved caspase-3
g
Relative miR-132 Level
350
300
250
200
150
100
50
0
*
CMV-eGFP
CMV-miR-132-eGFP
h
CMV-eGFP
i
CMV-miR-132-eGFP
j
BrdU+ cells (fraction of total cells)
1.E+04
1.E+04
8.E+03
6.E+03
4.E+03
2.E+03
0.E+00
CMV-eGFP
CMV-miR-132 -eGFP
k
kDa
pro-caspase-9
cleaved caspase-9
cleaved caspase-3
γ-tubulin
50
40
30
20
50
CMV-eGFP
CMV-miR-132 -eGFP
l
Densitometric analysis of Proteins as in k (%)
240
220
200
180
160
140
120
100
80
60
40
20
0
***
**
pro-caspase-9
cleaved caspase-9
cleaved caspase-3

Figure 3

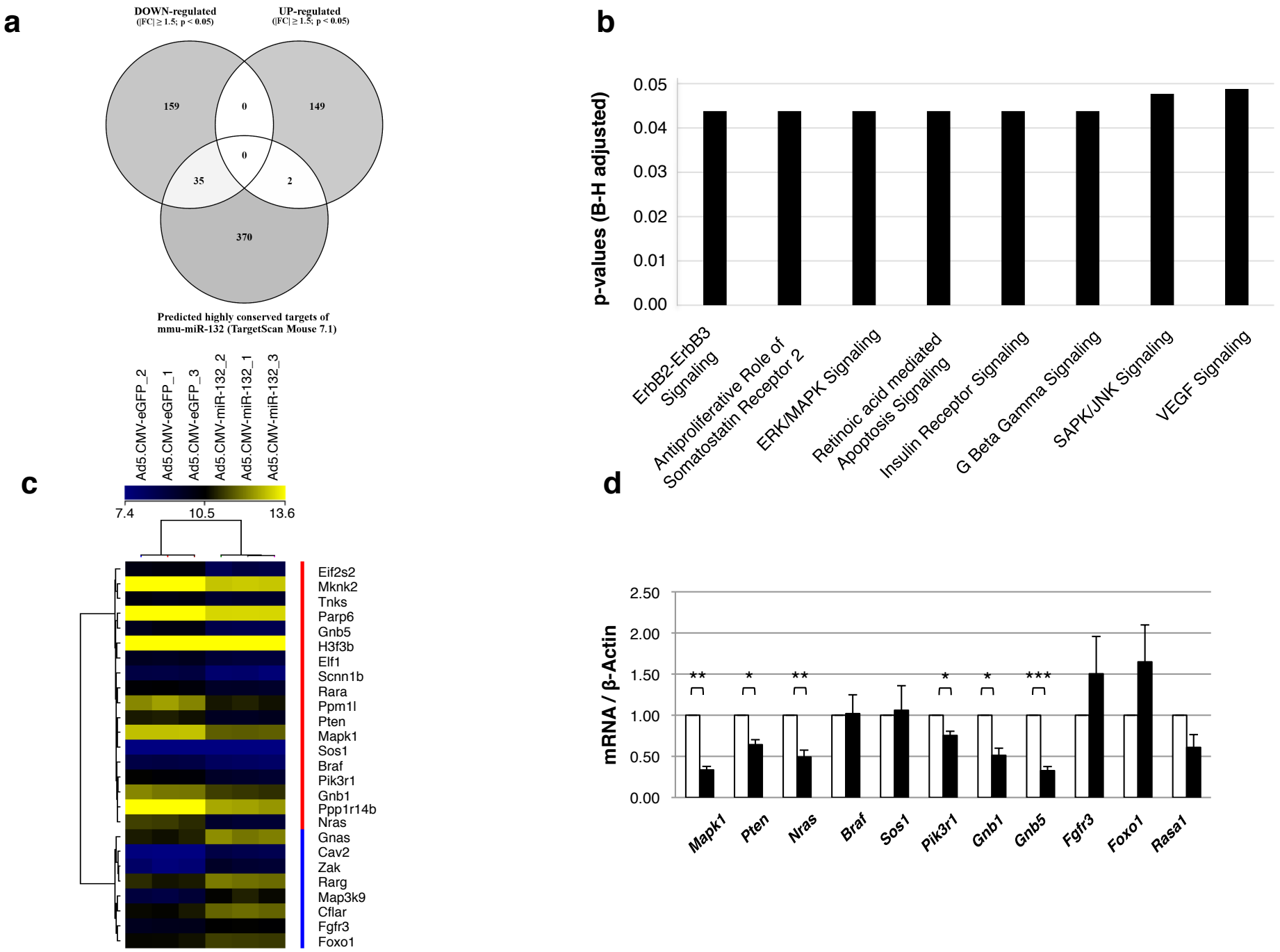
a
DOWN-regulated
(|FC| ≥ 1.5; p < 0.05)
UP-regulated
(|FC| ≥ 1.5; p < 0.05)
159
0
149
0
35
2
370
Predicted highly conserved targets of
mmu-miR-132 (TargetScan Mouse 7.1)
b
p-values (B-H adjusted)
0.05
0.04
0.03
0.02
0.01
0.00
ErbB2-ErbB3 Signaling
Antiproliferative Role of Somatostatin Receptor 2
ERK/MAPK Signaling
Retinoic acid mediated Apoptosis Signaling
Insulin Receptor Signaling
G Beta Gamma Signaling
SAPK/JNK Signaling
VEGF Signaling
c
Ad5.CMV-eGFP_2
Ad5.CMV-eGFP_1
Ad5.CMV-eGFP_3
Ad5.CMV-miR-132_2
Ad5.CMV-miR-132_1
Ad5.CMV-miR-132_3
7.4
10.5
13.6
Eif2s2
Mknk2
Tnks
Parp6
Gnb5
H3f3b
Elf1
Scnn1b
Rara
Ppm1l
Pten
Mapk1
Sos1
Braf
Pik3r1
Gnb1
Ppp1r14b
Nras
Gnas
Cav2
Zak
Rarg
Map3k9
Cflar
Fgfr3
Foxo1
d
mRNA / β-Actin
2.50
2.00
1.50
1.00
0.50
0.00
**
*
**
*
*
***
Mapk1
Pten
Nras
Braf
Sos1
Pik3r1
Gnb1
Gnb5
Fgfr3
Foxo1
Rasa1

Figure 4

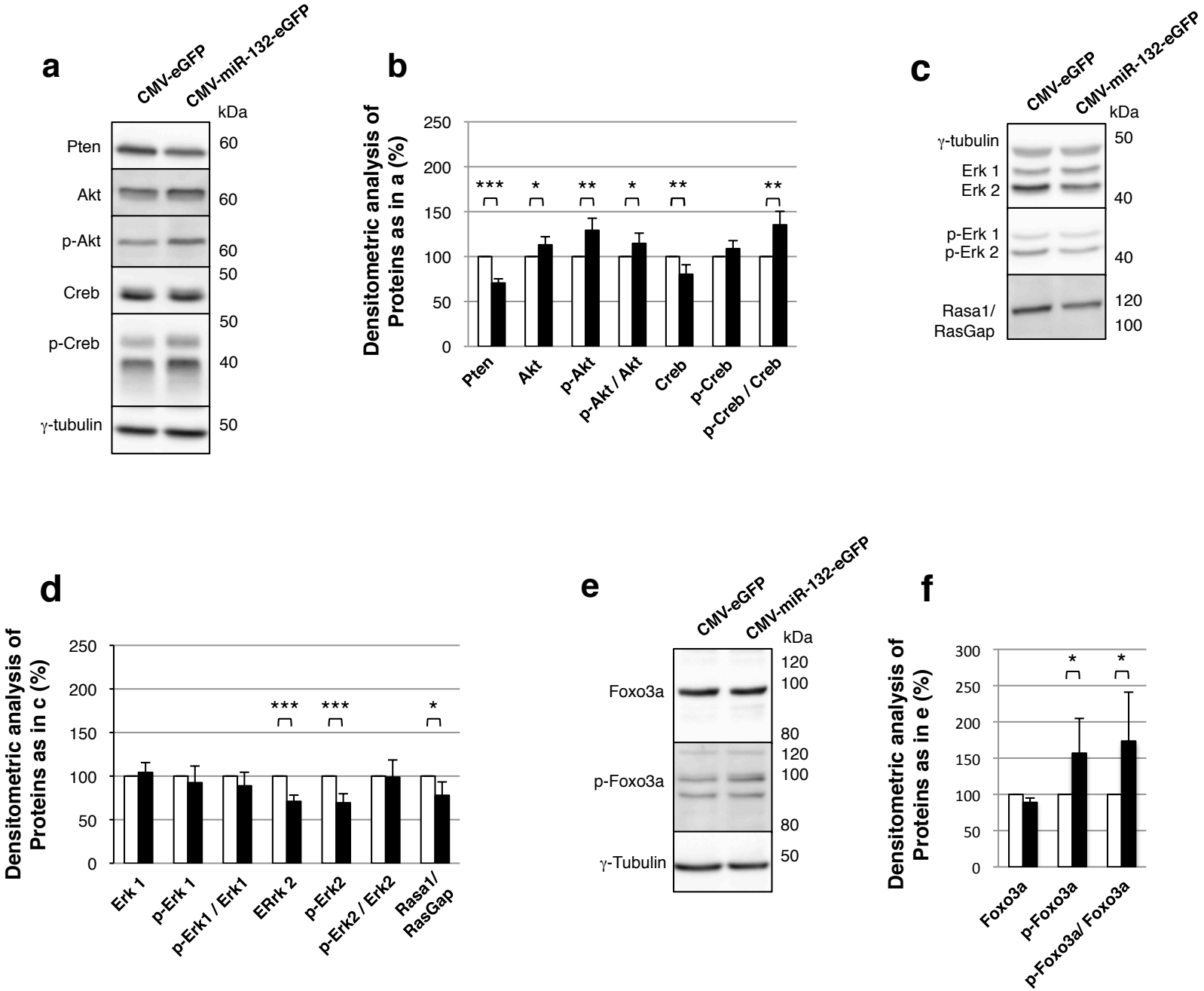
a
CMV-eGFP
CMV-miR-132-eGFP
kDa
Pten
Akt
p-Akt
Creb
p-Creb
γ-tubulin
60
60
60
50
50
40
50
b
Densitometric analysis of Proteins as in a (%)
250
200
150
100
50
0
***
*
**
*
**
**
Pten
Akt
p-Akt
p-Akt / Akt
Creb
p-Creb
p-Creb / Creb
c
CMV-eGFP
CMV-miR-132-eGFP
kDa
γ-tubulin
Erk 1
Erk 2
p-Erk 1
p-Erk 2
Rasa1/
RasGap
50
40
40
120
100
d
Densitometric analysis of Proteins as in c (%)
250
200
150
100
50
0
***
***
*
Erk 1
p-Erk 1
p-Erk1 / Erk1
ERrk 2
p-Erk2
p-Erk2 / Erk2
Rasa1/
RasGap
e
CMV-eGFP
CMV-miR-132-eGFP
kDa
Foxo3a
p-Foxo3a
γ-Tubulin
120
100
80
120
100
80
50
f
Densitometric analysis of Proteins as in e (%)
300
250
200
150
100
50
0
*
*
Foxo3a
p-Foxo3a
p-Foxo3a/ Foxo3a

Figure 5

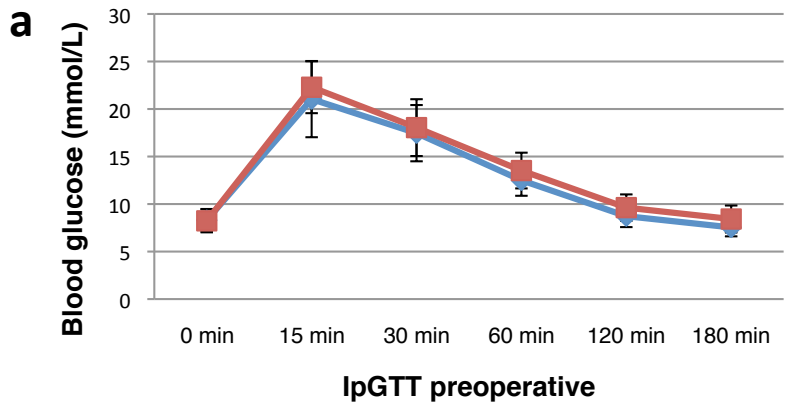
a
Blood glucose (mmol/L)
30
25
20
15
10
5
0
0 min
15 min
30 min
60 min
120 min
180 min
IpGTT preoperative

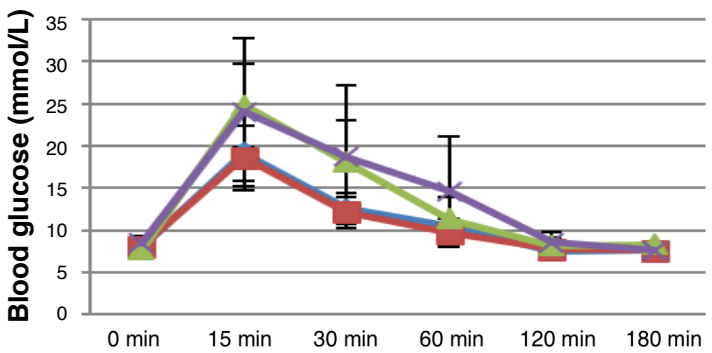
b
Blood glucose (mmol/L)
35
30
25
20
15
10
5
0
0 min
15 min
30 min
60 min
120 min
180 min

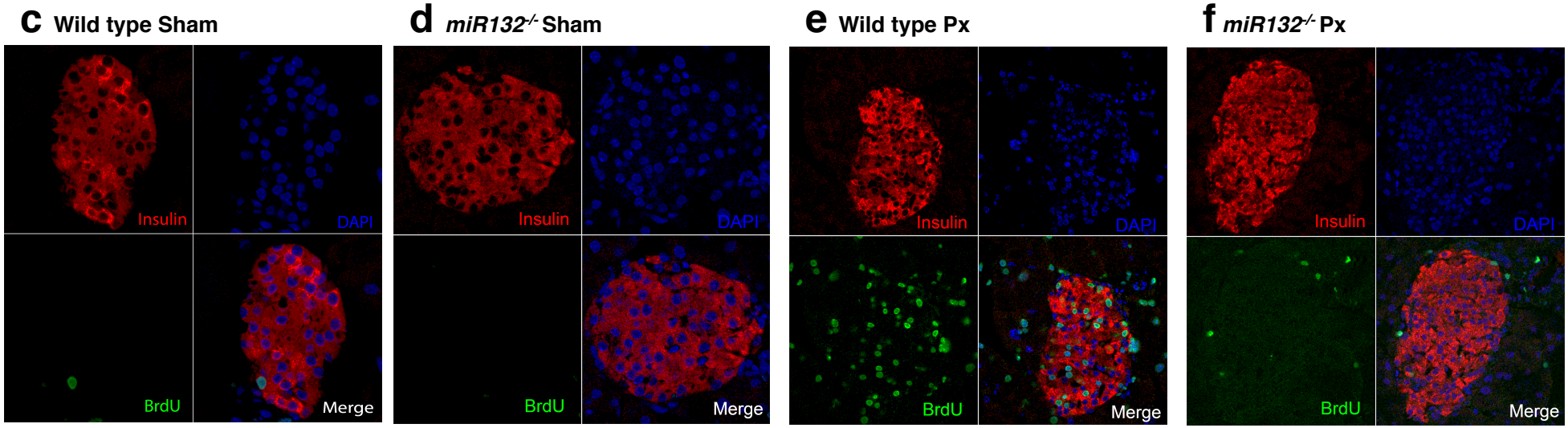
c Wild type Sham
d miR132-/- Sham
e Wild type Px
f miR132-/- Px
Insulin
DAPI
BrdU
Merge

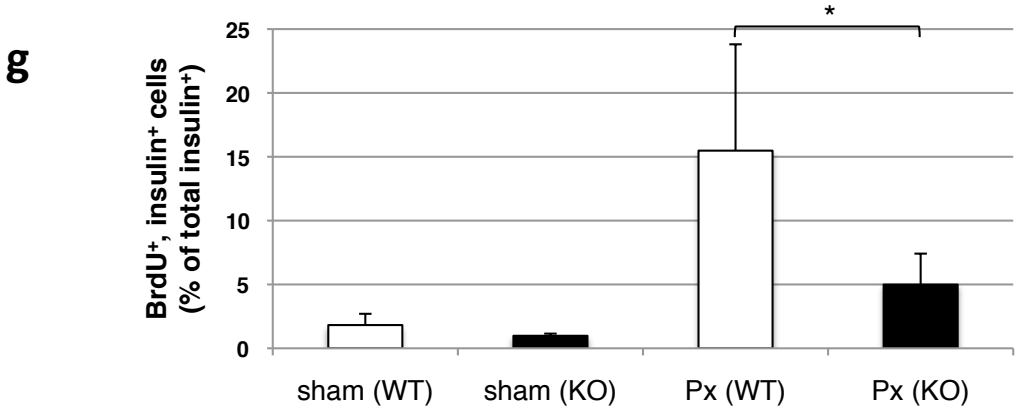
g
BrdU+, insulin+ cells
(% of total insulin+)
25
20
15
10
5
0
*
sham (WT)
sham (KO)
Px (WT)
Px (KO)

Table 1: miRNAs differentially expressed in islet cores of partially pancreatectomized mice ranked by fold change (absolute value)

Systematic name	p-value	FC	Px1	Px1	Px3	S1	S2	S3	S4
mmu-mir-205	0.009	4.91	6.5011	12.7521	9.4035	1	5.34742	2.0243	1
mmu-mir-132	0.005	4.63	85.442	90.0032	71.439	26.371	16.9079	22.282	8.6324
mmu-mir-186	0.016	2.5	4.0622	5.34086	3.1434	1.7227	1.1133	1.9388	1.686
mmu-mir-760	0.041	- 2.28	12.088	13.0156	4.6472	12.305	37.794	19.394	17.248
mmu-mir-129-3p	0.022	1.99	213.55	272.406	121.26	118.28	100.958	92.346	68.376
mmu-mir-690	0.03	1.79	49.413	48.5373	30.88	23.957	39.5096	16.126	17.206
mmu-mir-130b	0.014	1.77	42.937	40.5664	29.545	22.405	28.2766	18.247	14.679
mmu-mir-300*	0.045	1.77	2.9997	4.06448	2.006	1.8972	1.78003	1.8814	1
mmu-mir-598	0.049	1.75	18.357	22.9878	14.596	12.314	10.6534	12.703	6.3097
mmu-mir-431	0.013	1.65	23.393	27.3673	17.432	14.414	15.546	13.637	9.7251
mmu-mir-329	0.035	1.64	25.756	29.392	19.037	17.004	16.0322	15.797	9.9605
mmu-mir-154*	0.029	1.63	19.404	19.675	15.306	10.545	11.4188	13.067	8.2187
mmu-mir-141	0.04	1.59	878.04	970.708	655.42	566.11	672.314	515.55	318.15
mmu-mir-200c	0.039	1.58	976.04	997.919	672.69	608.97	681.16	530.91	361.34
mmu-mir-375	0.107	1.48	6291.99	7241.707	4643.13	4778.29	4398.79	4440.34	2461.28